Strength Analysis of Joints between Dissimilar Materials Using Interface Elements †

Hidekazu MURAKAWA*, Hisashi SERIZAWA**, Zhengqi WU*** and Masakazu SHIBAHARA****

Abstract

Crack propagation in both brittle and ductile materials and debonding along the interface in composite materials are typical examples of fractures. In these types of fractures, the failure is the consequence of surface formation accompanied by crack extension. Based on this understanding, the authors proposed an interface element which explicitly models the formation of new surfaces. The proposed method is applied to peeling of thin films from substrates, dynamic crack propagation in elastic materials and ductile crack growth. In this report, its applications to the strength analysis of elastic plate with a center crack and bonded joints between dissimilar materials are presented.

KEY WORDS: (Interface Element) (Finite Element Method) (Surface Energy) (Joint) (Crack Propagation) (Fracture) (Dissimilar Materials)

1. Introduction

The strength of a bonded joint is influenced by the geometry of the joint, the thickness of the adhesive, its elastic modulus and strength. Also, the roughness of the surfaces to be joined is influential. To study the influences of various parameters, the level of stress and the order of the singularity in the stress field are commonly employed for the relative evaluation of the strength. Although detailed information on the stress field is provided, little information on the criteria of the fracture is obtained from these types of study. This comes from the fact that, the physics of failure itself is not explicitly modeled in these analyses. The interface element which directly models the formation of the surface may have potential capability not only to give insight into the criteria of the fracture but also to make the quantitative prediction of strength itself.

2. Interface Potential

Essentially, the interface element is the distributed nonlinear spring existing between surfaces forming the interface or the potential crack surfaces as shown by **Fig.1**. The relation between the opening of the interface δ and the bonding stress σ is shown in **Fig.2**. When the opening δ is small, the bonding between two surfaces is maintained. As the opening δ increases, the bonding stress σ increases till it becomes the maximum value σ_{cr}. With further increase of δ, the bonding strength is rapidly lost and the surfaces are completely separated. Such interaction between the surfaces can be described by the interface potential. There are rather wide choices for this potential. The authors employed the Lennard-Jones type potential because it explicitly

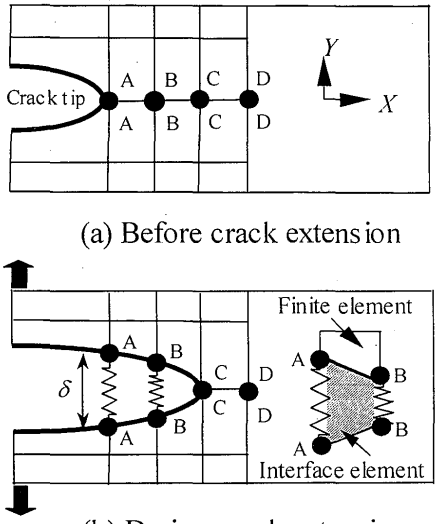

(a) Before crack extension

(b) During crack extension

Fig.1 Representation of crack extension using interface element.

† Received on December 18, 2000
* Associate Professor
** Research Associate
*** Dynus Co., Ltd.
**** Graduate Student, Osaka University

Transactions of JWRI is published by Joining and Welding Research Institute of Osaka University, Ibaraki, Osaka 567-0047, Japan.

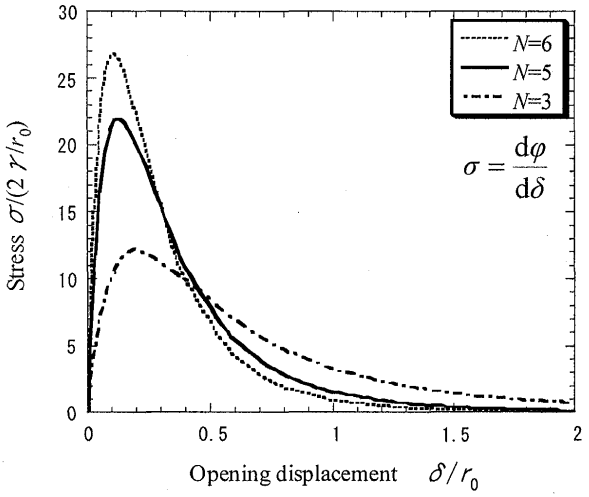

Fig.2 Relation between crack opening displacement and bonding stress.

involves the surface energy γ which is necessary to form new surfaces. Thus, the surface potential per unit surface area ϕ can be defined by the following equation.

$$\phi(\delta) = 2\gamma \cdot \left\{ \left(\frac{r_0}{r_0 + \delta} \right)^{2N} - 2 \cdot \left(\frac{r_0}{r_0 + \delta} \right)^{N} \right\} \tag{1}$$

where, constants γ, r_0, and N are the surface energy per unit area, the scale parameter and the shape parameter of the potential function. The derivative of ϕ with respect to the opening displacement δ gives the bonding stress σ acting on the interface,

$$\sigma = \frac{\partial \phi}{\partial \delta} = \frac{4\gamma N}{r_0} \cdot \left\{ \left(\frac{r_0}{r_0 + \delta} \right)^{N+1} - \left(\frac{r_0}{r_0 + \delta} \right)^{2N+1} \right\} \tag{2}$$

As it is seen from the above equation, the bonding stress σ is proportional to the surface energy γ and inversely proportional to the scale parameter r_0.

By arranging such interface elements along the crack propagation path as shown in Fig.1, the growth of the crack under the applied load can be analyzed in a natural manner. In this case, the decision regarding crack growth based on the comparison between the driving force and the resistance as in conventional methods is not necessary.

3. Influence of Parameters

Among three parameters involved in the interface energy function, only the surface potential γ has a clear physical meaning, while those of the scale parameter r_0 and the shape parameter N are not very clear. To clarify the influence of these parameters on the numerical results of failure problems, two simple problems are analyzed. One is the peeling of two bonded elastic strips and the other is the brittle fracture of an elastic plate with a center crack under tensile load. **Figure 3** shows the model for the peeling test. The process of peeling test is analyzed for different values of the scale parameter r_0

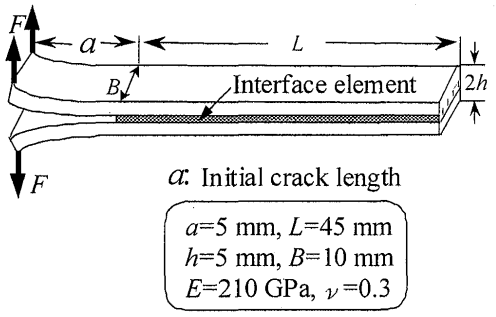

Fig.3 Peeling of bonded elastic strip.

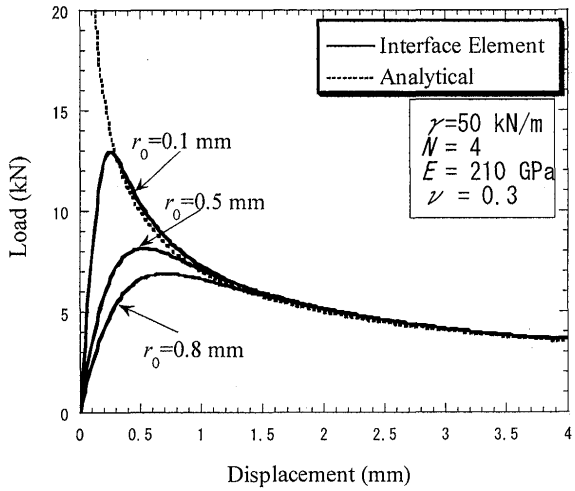

Fig.4 Effect of scale parameter r_0 on load-displacement curve.

while keeping the surface energy, γ, constant. The computed load-displacement curves are shown in **Fig.4**. The peak point of the curve corresponds to the start of peeling and the load decreases with the increase of peeling length. As seen from Fig.4, the scale parameter r_0 has some influence on the start of the peeling but it has almost no influence on the peeling process. Though it is not shown here, the shape parameter N and the mesh division have, no influence on the peeling process and the process is mainly governed by the surface energy γ[1,2]. For the quantitative assessment of the proposed interface element, the analytical solution is also plotted in the figure. The analytical solution of the present problem is given by the following equation.

$$F = \left(\frac{2EB^4h^3\gamma^3}{27} \right)^{\frac{1}{4}} \sqrt{\delta} \tag{3}$$

where, E, B, h are the Young's modulus, the breadth and the thickness of the strip, respectively. Good agreement with the analytical solution proves the capability of the proposed method for quantitative prediction.

In the same manner, the brittle fracture of the elastic plate with a center crack shown in **Fig.5** is analyzed. The plate is loaded through the vertical displacement given on both ends of the plate. In the serial computations, the

influence of the scale parameter r_0 is examined. The value of the surface energy γ is fixed as 2 kN/m and the value of the scale parameter r_0 is changed from 0.2 to 10 μm. One half of the plate is divided into 40×40 and 80×80 meshes as shown in **Fig.6**. The size of the element is reduced as the geometric series with ratio R. As the ratio R becomes small, the mesh division near the crack tip becomes fine. The effect of mesh size is examined by serial computations with R = 0.8, 0.7 and 0.6. **Figures 7** shows the load-displacement curve in case of R = 0.8 and r_0 = 0.2, 0.5, 2.0, 5.0, 10 μm, respectively. Similarly, **Fig.8** shows the relation between the opening displacement at the crack tip and the applied load. When the scale parameter is large such as the case with r_0 = 2.0 μm, stable crack growth is observed just after the maximum load and the computation stops due to the loss of stability. When the scale parameter is small, the instability occurs suddenly without a clear increase of the opening displacement or the drop of load. The load at the loss of stability is defined as the point of fracture.

The influence of the scale parameter and the mesh division on the fracture load is summarized in **Figs.9** and **10** with logarithmic and linear scales, respectively. For comparison, the fracture load computed using the analytical formula are shown in the figures. As is clearly seen from the figures, the curves can be divided into three parts with respect to the size of the scale parameter r_0. When r_0 is between 1.0 μm and 10 μm, the fracture load is almost independent of the scale parameter and the value is almost the same as the analytical value. When the scale parameter is smaller or larger than this range, the slope of the curve becomes -1. This can be explained in the following way. The middle part corresponds to the brittle fracture of the elastic plate with crack growth. Thus, the critical load is determined only by the surface energy γ and is independent of r_0 or the mesh division. According to Eq.(2), the bonding strength and the rigidity of the interface become small with an increase of the scale parameter. Therefore, the plate breaks in the separation mode without significant deformation of the plate or crack growth when the scale parameter is large. On the other hand, bonding strength becomes larger than the stress induced at the crack tip in the FEM model, when the scale parameter is small. In this case, the instability is not governed by the surface energy γ but by

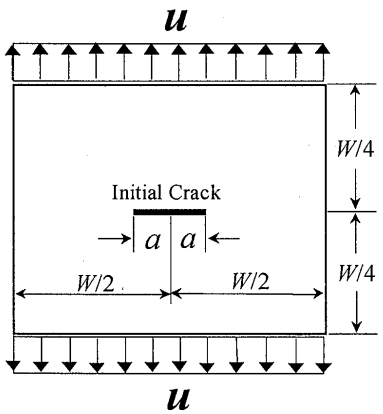

Fig.5 Elastic plate with center crack.

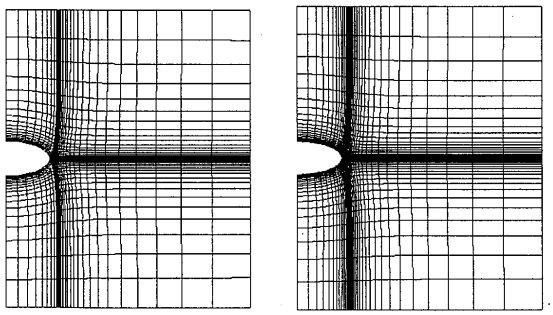

Fig.6 Mesh divisions superposed on deformation.

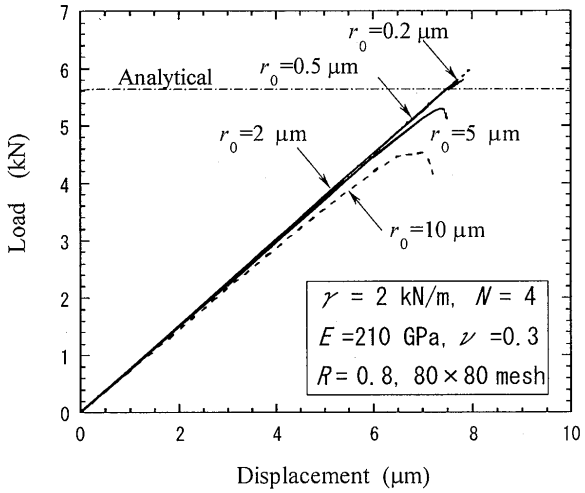

Fig.7 Load-displacement curve of elastic plate with center crack.

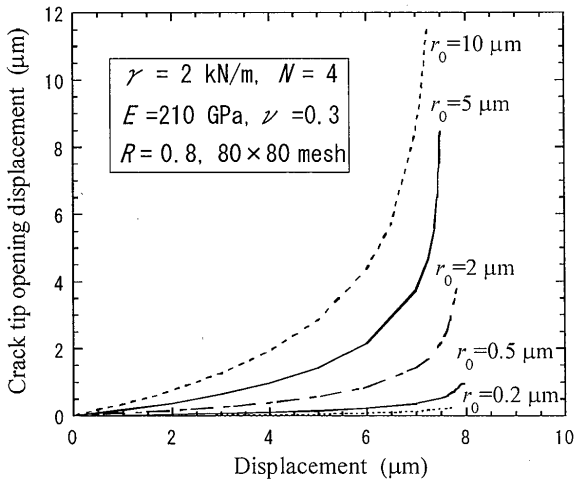

Fig.8 Applied displacement-crack tip opening in elastic plate with center crack.

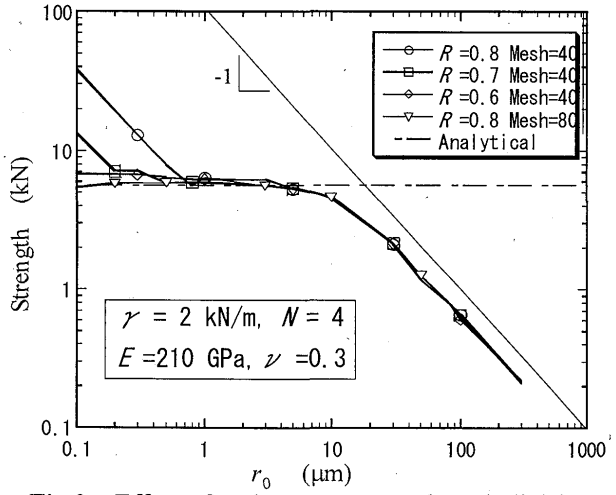

Fig.9 Effect of scale parameter and mesh division on predicted strength of elastic plate with center crack (logarithmic scale).

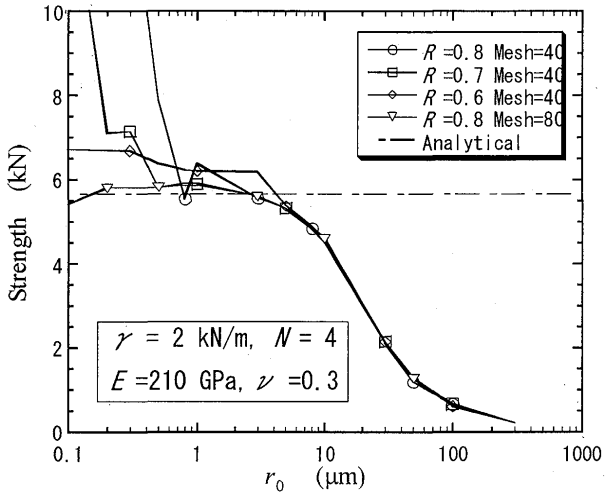

Fig.10 Effect of scale parameter and mesh division on predicted strength of elastic plate with center crack (linear scale).

the bonding strength σ_{cr}. At the same time this implies that the instability depends on the mesh division.

These computed results clearly show that the failure mode and the stability limit depend on the combination of the deformability of the plate and the mechanical properties of the interface.

4. Strength of Joint between Steel and Resin

As an example of a joint between dissimilar materials, co-cured joints between steel and resin as shown in **Figs.11** and **12** are analyzed. The length, the width and the thickness are 240 mm, 20 mm and 1 mm, respectively. Through the serial computations, the effect of scarf angle on the strength of the joint is investigated. Since the mode of the failure is mixed mode, the mechanical properties of the interface element need to be defined for both the opening and the shear modes. Although, an interaction between the two modes is expected, only the case when they are independent is reported for the lack of space. Their interaction will be reported elsewhere. According to this assumption, the interface potential ϕ can be defined as a sum of those for the opening mode ϕ_n and the shear mode ϕ_t as in the following equations.

$$\phi(\delta_n, \delta_t) = \phi_n(\delta_n) + \phi_t(\delta_t) \tag{4}$$

$$\phi_n(\delta_n) = 2\gamma_n \cdot \left\{ \left(\frac{r_{0n}}{r_{0n}+\delta_n} \right)^{2N} - 2 \cdot \left(\frac{r_{0n}}{r_{0n}+\delta_n} \right)^{N} \right\} \tag{5}$$

$$\phi_t(\delta_t) = 2\gamma_t \cdot \left\{ \left(\frac{r_{0t}}{r_{0t}+\delta_t} \right)^{2N} - 2 \cdot \left(\frac{r_{0t}}{r_{0t}+\delta_t} \right)^{N} \right\} \tag{6}$$

where, δ_n and δ_t are the opening and the shear deformation of the interface. Due to the symmetry of the shear deformation, the interface potential for the shear mode ϕ_t is assumed as a symmetric function of the shear deformation δ_t as shown in **Fig.13**.

In the serial computations, the Young's moduli E_s, E_r and Poisson's ratios ν_s, ν_r for the steel and the resin are

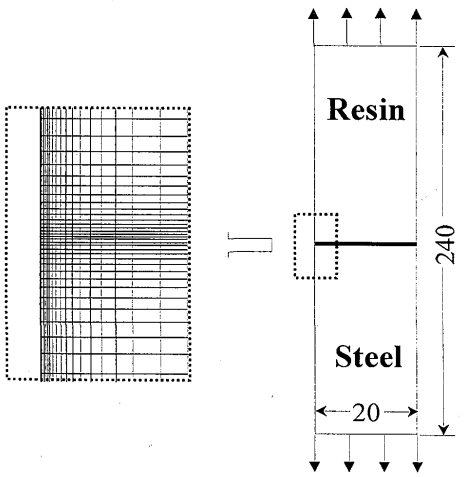

Fig.11 Model and mesh division of co-cured joint between steel and resin (θ= 90 degree).

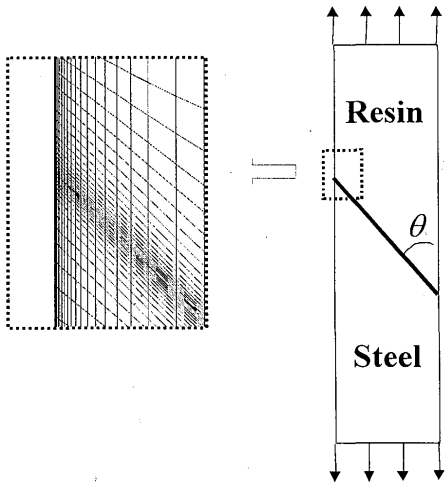

Fig.12 Model and mesh division of co-cured joint between steel and resin (θ= 45 degree).

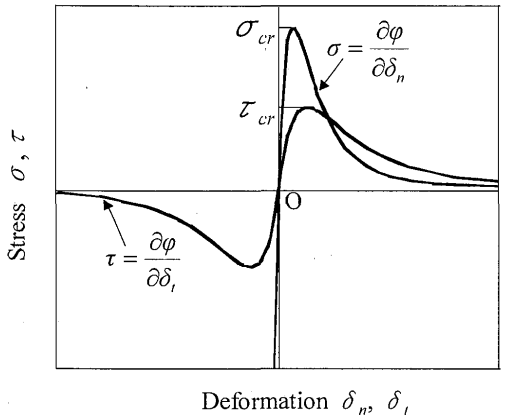

Fig.13 Displacement-stress relation at interface for opening and shear modes.

assumed to be 210 GPa, 5 GPa, 0.3 and 0.33, respectively. The surface energies γ_n, γ_t are kept constant and the scale parameters r_{0n}, r_{0t} are varied, i.e. $\gamma_n = \gamma_t = 2$ N/m and $r_{0n} = r_{0t} = 10^{-9} \sim 10^{-5}$ m. The scarf angle is also varied between 30 and 150 degree. The influence of the scale parameter and the scarf angle on the computed strength of the joints are summarized in **Figs.14** and **15**. The relation between the strength and the scale parameter is shown with a logarithmic scale in Fig.14. As opposed to the case of a cracked body discussed in the preceding section, the horizontal part is not observed in the case of joints between dissimilar materials. This means the strength of the joint is not determined by the surface energies γ_n, γ_t alone. It is determined by both the surface energy and the bonding strength σ_{cr}. When the slope is close to -1, the joint strength is strongly influenced by the bonding strength, while, the surface energy becomes influential when the slope is small. It is worth noting that the slope changes with the scarf angle. To closely examine the influence of the scarf angle, the relation between the joint strength and the scarf angle is summarized in Fig.15. The strength of the joint becomes small when the scarf angle is around 90 degree. Though the strength of the joint is not determined by the order of the singularity in stress field, this result suggests a strong relation between strength of the joint and the order of the singularity[3].

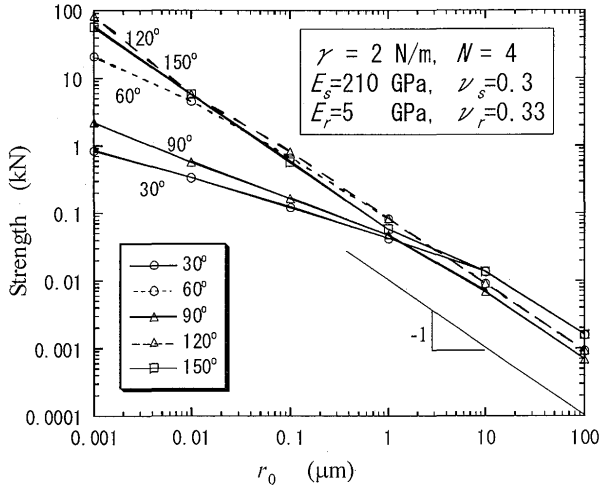

Fig.14 Influence of scale parameter r_0 on predicted strength of bonded joint.

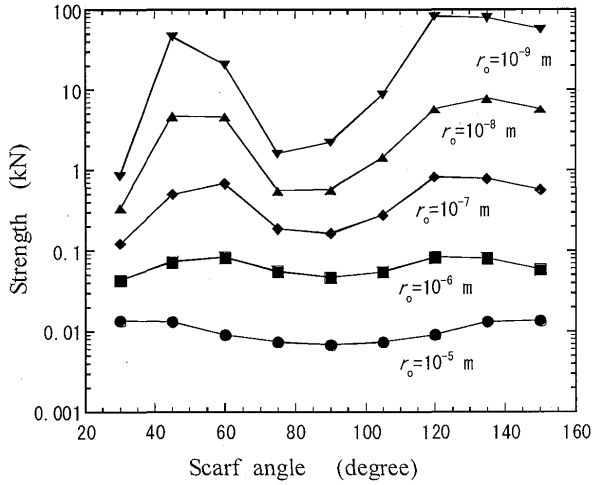

Fig.15 Influence of scarf angle on predicted strength of bonded joint.

5. Conclusions

The interface element is proposed as one of the simple models which represent the mechanism of failure in an explicit manner. It is applied to the analyses of the fracture strength of plate with an initial crack and the co-cured joints between steel and resin. The serial computations show that the mode of failure changes depending on the combination of the material property in bulk and that of interface. In case of an elastic plate with a center crack, the computed fracture load agrees fairly well with the analytical solution when the failure mode is crack growth type. In case of the joint between dissimilar materials, it is clearly shown that the strength is governed both by the surface energy and the bonding strength. As is demonstrated through these examples, the proposed method has a great potential as a tool to study the failure problems of various structures.

References

1) Z.Q.Wu, H.Serizawa and H.Murakawa : New Computer Simulation Method for Evaluation of Crack Growth Using Lennard-Jones Type Potential Function, Key Engineering Materials, Vol.166, pp.25-32 (1999).
2) Z.Q.Wu, H.Serizawa and H.Murakawa : Computer Simulation Method for Crack Growth Using Interface Energy and Its Application to Interface Stripping of Composite Material (2nd Report), No.232, pp.145-153 (1999-9) (in Japanese).
3) Y.Ito, T.Shindoh, H.Andoh and K.Nagata : Effect of Interface Shape on the Strength for Carbon Steel / PMMA Adhered Joint, J. Soc. Mat. Sci., Japan, Vol.48. No.3, pp.264-268 (1999-3) (in Japanese).